

X-Ray Spectrum of the BL Lacertae Object PKS 2155–304

Takaya OHASHI and Kazuo MAKISHIMA

*Department of Physics, Faculty of Science, The University of Tokyo,
3-1, Hongo 7-chome, Bunkyo-ku, Tokyo 113*

Hajime INOUE, Katsuji KOYAMA,* and Fumiyoshi MAKINO

*Institute of Space and Astronautical Science,
1-1, Yoshinodai 3-chome, Sagami-hara-shi, Kanagawa 229*

and

Martin J. L. TURNER and Robert S. WARWICK

*X-Ray Astronomy Group, Department of Physics, University of Leicester,
Leicester, LE1 7RH, U.K.*

(Received 1988 September 9; accepted 1989 February 9)

Abstract

The BL Lacertae object PKS 2155–304 was observed with Ginga for two days in May 1987. The 2–35 keV intensity showed a significant variability, the most rapid change being a 30% increase in 3 hr. The X-ray spectrum was described by a single power-law model with photon spectral index ranging between 2.7 and 2.9, but the power-law slope showed no clear correlation with the intensity level and stayed at a similar value for each day. No significant iron emission line ($EW < 50$ eV) nor iron K absorption edge ($N_{\text{Fe}} < 2 \times 10^{17} \text{ cm}^{-2}$) was observed. The high-quality spectrum observed with Ginga up to 35 keV has revealed no significant hard tail. The 90% upper limit on the flux of the flat hard tail is $0.3 \mu\text{Jy}$ at 20 keV, less than half of the previously reported level. The present spectral results combined with the previously observed fast variability constrain the emission mechanism of PKS 2155–304; a simple homogeneous synchrotron self-Compton model is difficult to explain the whole emission spectrum, suggesting an inhomogeneous geometry in the emission region.

Key words: Active galactic nuclei; BL Lacertae objects; Spectra of X-ray sources.

1. Introduction

The spectra of BL Lac objects are generally characterized by a featureless

* Present address: Department of Astrophysics, School of Science, Nagoya University, Furo-cho, Chikusa-ku, Nagoya 464-01.

continuum extending from the radio to the X-ray region (Stein et al. 1976). Significant polarization has been observed in the radio and optical bands, indicating that synchrotron emission is probably the dominant process at least at these wavelengths. However, in the X-ray region where polarization measurements are not available, the emission mechanism (direct synchrotron or Compton scattering) and the cause of variability is uncertain. The rapid variability often observed in BL Lac objects suggests that, at least in some sources, the emission may be strongly beamed towards the observer.

PKS 2155–304 is one of the brightest and the most variable BL Lac objects in the X-ray band with a redshift of 0.117 (Bowyer et al. 1984). The X-ray variability of the source has been observed from various satellites (Snyder et al. 1980; Morini et al. 1986; Agrawal et al. 1987). In particular, recent observations from EXOSAT have shown that the intensity in 1–6 keV band varied by a factor of 4 in 4 hr (Morini et al. 1986). If the X-ray emission is isotropic, such a fast variability violates the theoretical efficiency limit for known emission processes (e.g., Cavallo and Rees 1978; Fabian 1979).

In the X-ray band the spectrum of PKS 2155–304 is well approximated by a power-law model with photon spectral index of 2.5–3 (see Urry 1986). However, various features have been detected in the previous spectral measurements. First, a flat hard tail was observed above 10 keV with HEAO-1 in 1978 (Urry and Mushotzky 1982) with an intensity of about $0.8 \mu\text{Jy}$ at 20 keV, which has been interpreted as a Compton upscattered component in the synchrotron self-Compton (SSC) model. Urry and Mushotzky (1982) discuss the overall spectrum from radio to X-rays in terms of an SSC model with relativistic beaming of the X-ray emission. [But see also Ghisellini et al. (1985), who show that relativistic beaming is not necessary for inhomogeneous SSC emission from a jet.] Second, a sharp absorption trough in the low energy spectrum was observed with the grating spectrometer (OGS) on the Einstein Observatory (Canizares and Kruper 1984). This feature occurred between 600 and 700 eV, and has been interpreted as O VIII Ly α absorption by a hot outflowing gas (Canizares and Kruper 1984; Krolik et al. 1985). The solid state spectrometer on the Einstein Observatory revealed an apparent low-energy absorption corresponding to $N_{\text{H}} = 1.3 \times 10^{21} \text{ cm}^{-2}$, which exceeds both the column density within our galaxy ($N_{\text{H}} = 5 \times 10^{20} \text{ cm}^{-2}$) and the IPC-measured N_{H} (Madejski 1985) and may therefore be due to “warm” matter intrinsic to the source (Urry et al. 1986).

Observations of the UV spectrum of PKS 2155–304 by IUE over many years have shown that the UV power-law energy index changes between 0.6–1.3, and there is no correlation between the intensity and spectral index (Maraschi et al. 1986; Urry et al. 1988).

In order to understand the emission mechanism and the geometry of emitting regions in BL Lac objects, it is highly desirable to observe the spectrum and its variability with improved sensitivity. The LAC instrument on board the third Japanese X-ray astronomy satellite Ginga (Makino and the ASTRO-C team 1987) has a very large (4000 cm^2) effective area and a wide spectral response (2–37 keV) with superior background rejection efficiency (Turner et al. 1989). We observed PKS 2155–304 for two days in May 1987 during the test period of Ginga. In this paper we report on the properties of the X-ray spectrum of PKS 2155–304 based on the high-quality data

obtained with Ginga.

2. Observations

Observations of PKS 2155–304 were carried out on 26 and 27 of May, 1987. On each day, the source was observed for typically 20 min per satellite orbit, the orbital period being 96 min, and for ten orbits per day. These ten orbits correspond to those when the satellite loses ground contact (remote orbits), during which the LAC background count rate is generally low and stable (Hayashida et al. 1989). The observing window in each orbit is chosen where the background is lowest.

The background was observed on May 25 with the detector f.o.v. pointing towards a “blank” sky near the Small Magellanic Cloud. Both PKS 2155–304 and the background position have galactic latitude greater than 40° , and therefore the effect of galactic emission (Koyama et al. 1986) is negligible. In fact, we have confirmed that the observed X-ray intensity in this background position agrees with the average sky background discussed by Hayashida et al. (1989). So there is no significant contamination from discrete X-ray sources in the background data.

MPC-1 mode was used throughout the observations. This enables us to obtain pulse-height spectra in 48 channels for individual detector layers with time resolution of 16 s. The counting rate of the medium layer below 8 keV is insensitive to incident X-rays and provides a good measure of non-X-ray background. The method of the background subtraction is briefly described by Turner et al. (1989). The uncertainty due to the background subtraction process is a few times $10^{-2} \text{ counts s}^{-1} \text{ keV}^{-1}$ ($\sim 10^{-5} \text{ counts cm}^{-2} \text{ s}^{-1} \text{ keV}^{-1}$).

3. Results

3.1. Intensity and Spectral Variations

The observed intensity of PKS 2155–304 averaged over the typically 20-min interval of observation in four different energy bands are plotted as a function of time in figure 1. In this analysis data recorded during high-background conditions [with $\text{SUD} > 6.2 \text{ counts s}^{-1} \text{ detector}^{-1}$, where SUD is the detector counting rate above 37 keV and is used as a measure of the non-X-ray background level; see Turner et al. (1989)] are excluded. The average flux is $5.0 \mu\text{Jy}$ in the 2–10 keV band, but variations of 30–40% are observed in all energy bands. The intensity variation shows a similar pattern on both days, but we can conclude that the observed variation is intrinsic to the source for the following reasons:

1. In the 1.7–4.0 keV band the intensity change is a factor of ~ 100 larger than the systematic error in the background subtraction, and even in the higher energy band (9.8–15 keV) this factor is nearly 10.
2. We applied the same analysis method on the background data taken on the previous day and found no significant systematic variation.
3. The pulse-height spectrum is well fitted by a power-law model at all intensity levels for the entire energy range 2–37 keV. If the observed variation is due to an

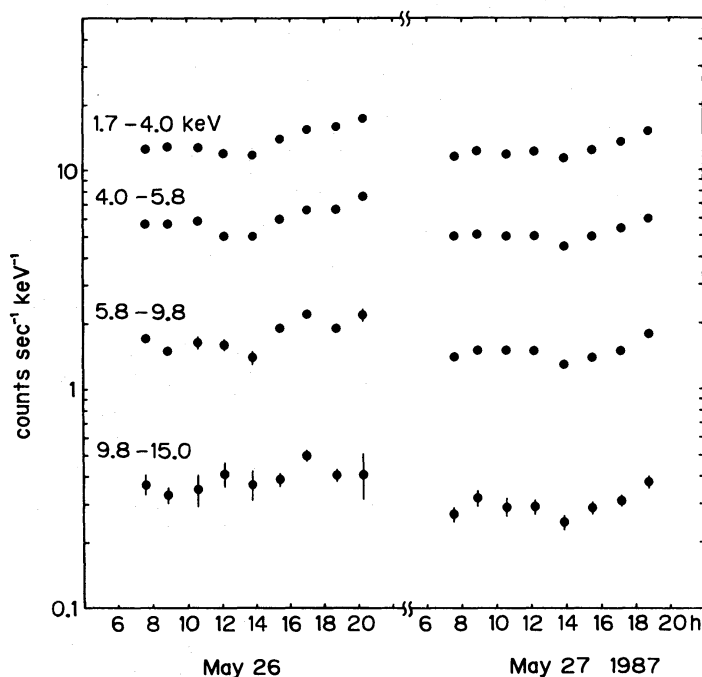


Fig. 1. The light curve of PKS 2155–304 in four energy bands. Each data point corresponds to an observation for typically 20 min.

incorrect background subtraction, the spectrum should show contamination by a flat spectral component (produced by the non X-ray background).

The fastest variation occurred between 14h and 17h on May 26, when the luminosity of PKS 2155–304 in the 2–30 keV range increased from $3.1 \times 10^{45} \text{ erg s}^{-1}$ to $4.1 \times 10^{45} \text{ erg s}^{-1}$ in 3 hr assuming isotropic emission.

The spectrum from each ~ 20 -min observation can be fitted with a simple power-law model as mentioned above. We determined the spectral index in each interval assuming N_{H} to be $1.3 \times 10^{21} \text{ cm}^{-2}$ after Urry et al. (1986) and we looked for correlation with the source flux. Figure 2 shows the result. The plotted errors are 90% confidence limits for a single parameter (i.e., $\chi^2_{\text{min}} + 2.7$ with all “other” parameters readjusted to minimize the χ^2). There is a significant variation in the spectral index, but the correlation between the intensity and the spectral index is poor. The data indicate that the photon index stays at roughly constant value in each day, i.e., it is around 2.7 on May 26 and 2.8 on May 27, respectively, despite relatively large change in intensity.

3.2. Energy Spectrum

In order to study the X-ray spectrum of PKS 2155–304 in detail, the data from each day have been combined together since the spectral index stays almost constant within each day. The effective observation time was 5002 s and 5760 s on May 26 and 27, respectively.

Figures 3a and b show the pulse-height spectrum of PKS 2155–304 for each day fitted with a power-law model. The fit with the simple power-law model with neutral absorbing gas is good. The χ^2 values are 21.8 and 26.1 for (a) and (b), respectively, for 26 degrees of freedom. The N_{H} values are less than $3 \times 10^{21} \text{ cm}^{-2}$, which is consistent

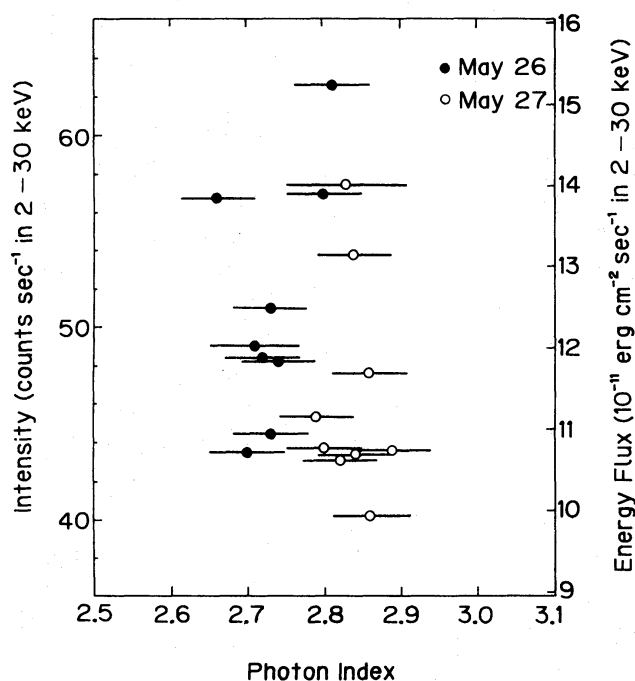


Fig. 2. Correlation between the X-ray intensity and the photon index derived from the spectral fittings with N_{H} fixed at $1.3 \times 10^{21} \text{ cm}^{-2}$ after Urry et al. (1986). The filled and open circles are for May 26 and 27, 1987, respectively. Errors for the photon indices are single-parameter 90% errors. The approximate energy flux assuming a photon index of 2.8 is indicated in the right-side scale. The systematic error due to the difference in the photon index is less than 4%.

with $1.3 \times 10^{21} \text{ cm}^{-2}$ obtained with the Einstein SSS observation (Urry et al. 1986).

To investigate the possible curvature of the spectrum between low- and high-energy bands as suggested by Urry et al. (1986), each spectrum is divided at 9.8 keV and separately tested with a power-law model. We have fixed the N_{H} value at $1.3 \times 10^{21} \text{ cm}^{-2}$ in order to improve the sensitivity to a change in the spectral index.

The results are summarized in table 1. The statistical error (90% confidence) on the spectral index is typically 0.02 for 1.7–9.8 keV and 0.2 for 9.8–37 keV, respectively, however in table 1 we put larger errors by taking the systematic errors into account. The absolute value of the spectral index measured with the LAC may have a systematic error of about 0.04 based on the calibration with the Crab Nebula (Turner et al. 1989). We have included this error as a square sum to the statistical errors. For the energy band 9.8–37 keV, the background subtraction is a major source of the systematic error. We have studied this by comparing the results between the top and middle layers, and increased the errors so that the results of both layers become consistent with each other. This has the effect of making the fit parameters more uncertain and in that sense is a conservative procedure.

The results shown in table 1 indicate that no significant change of the spectral index is detected between the high- and low-energy bands.

We have also investigated possible iron absorption and emission features in the PKS 2155–304 spectrum. First, we assumed the energy of the iron absorption edge to be 6.36 keV, corresponding to that for neutral iron with a redshift 0.117 (Bowyer et al.

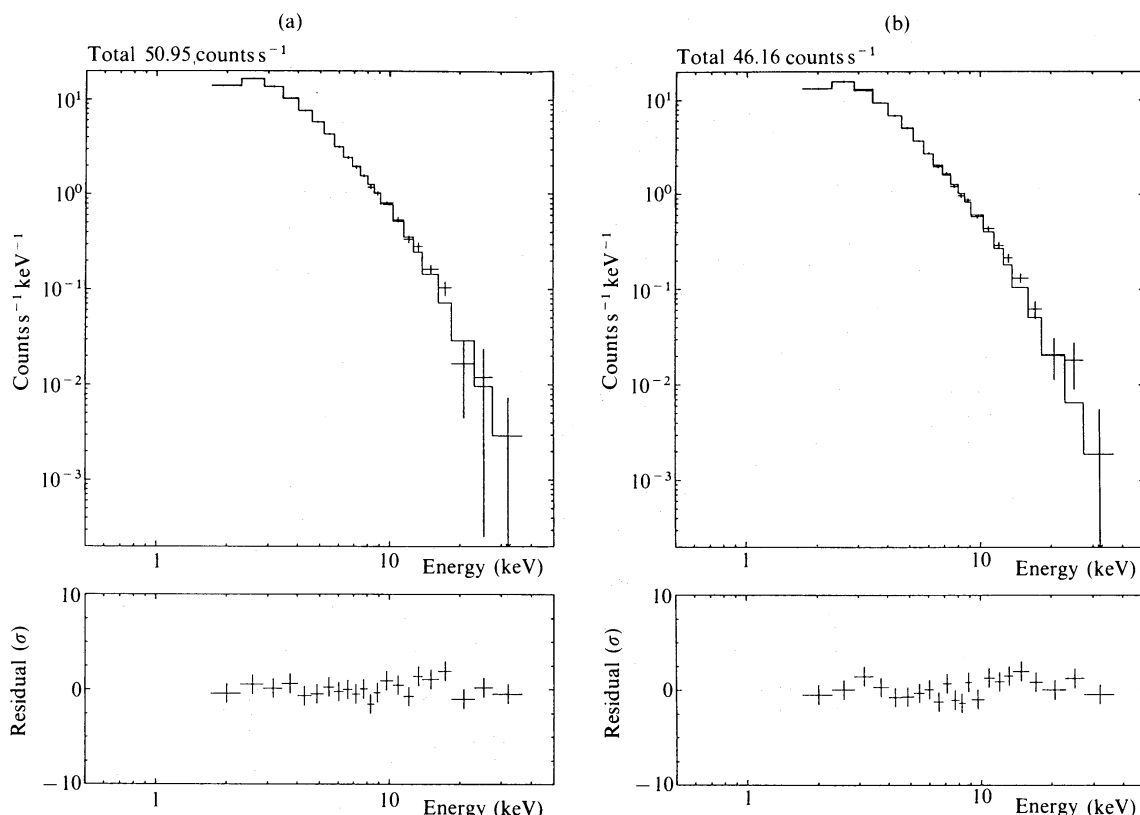


Fig. 3. Pulse-height spectra accumulated for (a) May 26 and (b) May 27, 1987, respectively. The best-fit power-law models are fitted to the data. The bottom panels indicate the residuals of the fit in units of σ .

Table 1. Spectral indices in high- and low-energy bands and column density of absorption edge.

Physical quantity	May 26	May 27
Photon index:		
1.7–9.8 keV	2.74 ± 0.05	2.84 ± 0.05
9.8–37 keV	2.61 ± 0.24	2.40 ± 0.40
Absorption edge (N_{Fe})	$< 1.8 \times 10^{17} \text{ cm}^{-2}$	$< 3.6 \times 10^{17} \text{ cm}^{-2}$

1984). As shown in table 1, only an upper limit, $N_{\text{Fe}} < 1.8 - 3.6 \times 10^{17} \text{ cm}^{-2}$, has been obtained. [But see also Treves et al. (1989).] This value indicates that if abundances are solar (e.g., Allen 1973) the amount of intervening cold gas intrinsic to the source is less than $5 \times 10^{21} \text{ cm}^{-2}$. This is consistent with the N_{H} values obtained with IPC by Madejski (1985) and with SSS by Urry et al. (1986). Secondly the upper limit for the equivalent width of a redshifted iron line (5.7 and 6.0 keV from neutral and helium-like irons, respectively) is 50 eV at 90% confidence. This is much smaller than the values (200–300 eV) for some AGNs for which significant iron lines are observed (Matsuoka et al. 1986; Wang et al. 1986; Ohashi 1988).

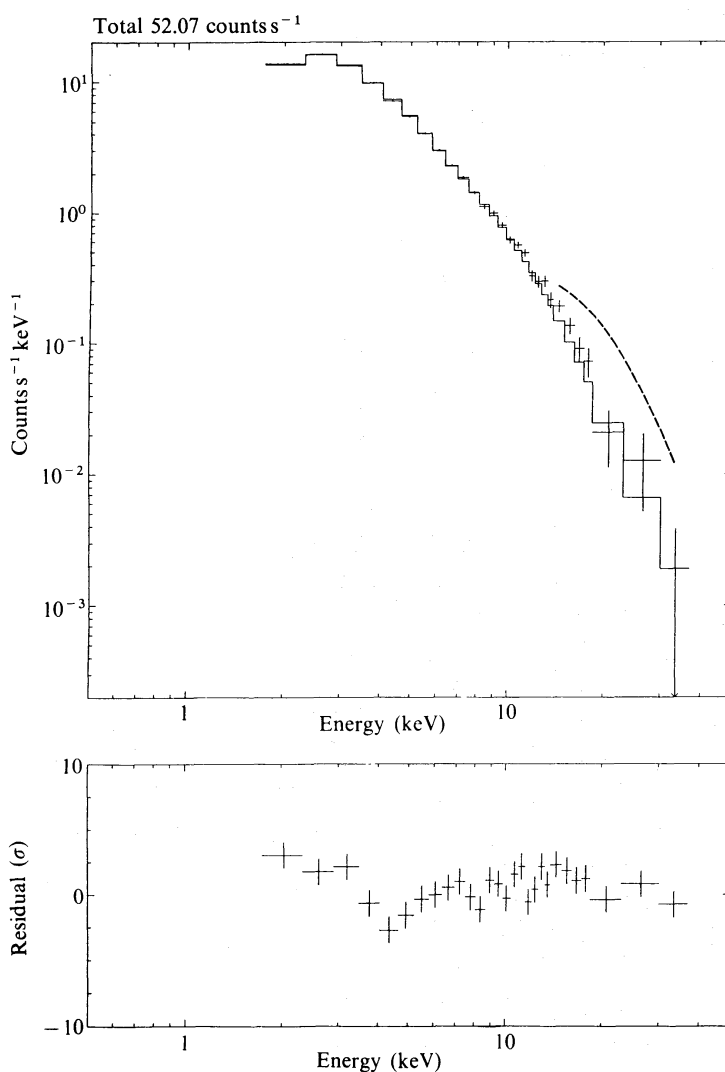


Fig. 4. Pulse-height spectra accumulated for all of the low-background observations ($\text{SUD} < 5.7 \text{ counts s}^{-1} \text{ detector}^{-1}$). No significant hard tail in excess of the best-fit power-law model is seen. An expected tail feature for $0.8 \mu\text{Jy}$ level is indicated with a dashed line. The bottom panel indicates the residual of the single power-law fit in units of σ .

3.3. Hard Tail

The data taken under very low background condition ($\text{SUD} < 5.7 \text{ counts s}^{-1} \text{ detector}^{-1}$) are all accumulated in order to check the presence of the hard tail. A combination of power-law spectra having different slopes gives a concave spectral shape (spectrum gets harder toward higher energies), but in the present data the variation range of the spectral slope is narrow (about 0.2 as shown in figure 2) and very different from the flat slope. Therefore, we neglect here the effect of the variation of spectral slope in the study of the flat hard tail. Figure 4 shows the combined pulse-height spectrum fitted with a single power law. Above 8 keV the fit with the single component power-law model is good with no systematic deviation at high energies.

We assumed a second component with flat incident spectrum (photon index equals to zero) and conducted a spectral fitting with a two-component spectrum. The free

parameters were the interstellar absorption, the intensity and photon index of the first power-law component, and the intensity of the flat component. The slope of the flat component was fixed. This analysis gave the intensity level of the flat spectrum to be less than $0.3 \mu\text{Jy}$ at 20 keV with 90% confidence. The upper limit value is less than half of the level ($0.8 \pm 0.2 \mu\text{Jy}$) observed with HEAO-1 A-2 by Urry and Mushotzky (1982). The expected hard tail feature for $0.8 \mu\text{Jy}$ level implies a factor of four higher flux at 20 keV than the level presently observed with Ginga. Note that the 2–10 keV flux of the source was $8.5 \pm 1.5 \times 10^{-11}$ and $9.7 \pm 0.5 \times 10^{-11} \text{ erg cm}^{-2} \text{ s}^{-1}$ for HEAO-1 and Ginga, respectively.

We need to check the possibility that the background subtraction process has suppressed the presence of the hard tail, which would occur only if we are using systematically too high a background throughout the analysis. To check this, the average SUD rate in the low background region taken on May 26 and 27 when PKS 2155–304 was in the f.o.v. has been compared with that on May 25 when the blank sky was observed. In fact the SUD levels agree well within 1%, implying that the background level from May 25 to 27 was constant within 1%. A change of the background by 1% results in a hard tail of less than $0.1 \mu\text{Jy}$ at 20 keV. Therefore, we conclude that there was no significant hard spectral component present in the spectrum of PKS 2155–304 in May 1987.

4. Discussion

The Ginga observation has provided a high-quality X-ray spectrum of PKS 2155–304 in the energy range 2–35 keV. During the two days of observation, PKS 2155–304 showed an intensity variation of $\sim 30\%$ ($\Delta L \sim 1 \times 10^{45} \text{ erg s}^{-1}$) in 3 hr. The rate of luminosity change, $\Delta L / \Delta t \sim 9 \times 10^{40} \text{ erg s}^{-2}$, is one order of magnitude smaller than that observed with EXOSAT in 1984 (Morini et al. 1986). We have searched for various discrete spectral features (such as emission lines, absorption edges, and spectral turnovers), but even with the sensitivity of Ginga we could derive only upper limits. The implications of these results are discussed below.

Canizares and Kruper (1984) detected a pronounced absorption feature at 600 to 700 eV with the Einstein Observatory OGS. This feature together with the revised measurement of the redshift by Bowyer et al. (1984) has been interpreted as due to the O VIII resonant line absorption. Krolik et al. (1985) argued that the depth of the iron K absorption edge will constrain the temperature of the outflowing gas responsible for the absorption line. The present upper limit of $N_{\text{Fe}} = 2 \times 10^{17} \text{ cm}^{-2}$ corresponds to an optical depth of $\tau_{\text{K}} = 0.007$. This implies that if we require simultaneously both the 0.6 keV absorption feature and no iron K edge, the temperature of the gas needs to be between about $3 \times 10^4 \text{ K}$ and $2 \times 10^5 \text{ K}$ so that the abundance of O VIII ion is near the maximum.

Fluorescent iron lines can provide a powerful probe to investigate the surrounding matter and the X-ray beaming from the central object in the active galactic nuclei (e.g. Inoue 1985). The 90% upper limit for the equivalent width (EW) of the iron K emission line (redshifted from 6.4 keV and 6.7 keV) is 50 eV for PKS 2155–304, consistent with the non thermal origin of the X-ray emission. Also, the X-ray flux is not irradiating

cool matter in the system, which is different from some Seyfert galaxies and quasars showing strong iron line features (Matsuoka et al. 1986; Ohashi 1988; Koyama et al. 1989).

We have performed spectral fitting for each of the data sets (20–30 min long) taken in individual satellite orbits. The result indicates that the spectral index varies significantly with time between 2.6 and 2.8, but no simple correlation is obtained between the intensity and the index. Morini et al. (1986) report that, in an EXOSAT observation of PKS 2155–304 in the 2–6 keV band, spectral hardening accompanied a dramatic intensity increase by a factor of 6. On the other hand, the extensive study of ultraviolet spectrum with IUE shows that the observed values of spectral index and intensity of PKS 2155–304 are uncorrelated (Urry et al. 1988).

So far the observational results for BL Lac sources have shown that the relation of spectral index to the intensity is complicated. The X-ray spectrum of Mrk 421 became steeper when the intensity decreased (Mushotzky et al. 1979), and a systematic correlation in the same direction has been reported by George et al. (1988). However, recent Ginga results show an almost constant spectral index of Mrk 421 for intensity levels different by a factor of nearly 3 (Ohashi and Makino 1988).

Let us consider the following simple situation. Assume that the X-ray emission is produced by a synchrotron process and that the X-ray variability is caused by the change in the injected electron flux. The magnetic field and electron spectrum are assumed to be constant with time for simplicity. In this case, the X-ray variability is controlled by the injected electron flux and also by the synchrotron loss. The synchrotron energy loss of the electrons is proportional to E^2 . This determines the slope of the equilibrium photon spectrum. For the same incident electron spectrum, the X-ray spectrum is flattest when synchrotron loss has negligible effect on electron energy, and it becomes steepest when synchrotron loss dominates the electron energy (Tucker 1975). However, if the source is observed just after an outburst (fresh injection of electrons), the high-frequency spectrum will be dominated by the young electrons which have not decayed yet and the spectrum will flatten (Kellermann 1966).

The X-ray intensity of PKS 2155–304 has decreased and increased by about 30% within several hours. Figure 2 shows that the spectral slope stays constant during such intensity change. Under the simple case described above, the observed features will imply following situations:

1. The synchrotron energy loss is faster than several hours, because the X-ray flux (assumed to be synchrotron radiation) cannot decrease faster than the synchrotron-loss timescale.
2. The fact that the X-ray spectrum stays constant for different intensities implies that the equilibrium spectrum is reached at all energies almost instantaneously (much faster than several hours).

The energy-loss time scale (τ) in terms of the radiated photon energy E_{ph} (keV) is given by (Tucker 1975)

$$\tau \sim 1000 B^{-1.5} E_{\text{ph}}^{-0.5} \text{ s},$$

where B (G) is the magnetic field in the emission region. A timescale less than 3 hr

corresponds to $B > 0.2$ G. The absence of significant spectral change during the intensity variation suggests that the magnetic field would be much stronger than this value. However, note that the present estimation neglects the effect of relativistic beaming. If more dramatic variability is observed, we can perform a better test of the simple emission models using the energy dependence of the variability.

The hard tail previously detected by HEAO-1 (Urry and Mushotzky 1982) was not observed in the present observation, the upper limit for a flat spectral component being less than 40% of the level observed by Urry and Mushotzky (1982). It is interesting to point out that except for the hard tail both the 2–10 keV intensity and the spectral slope are consistent between the two observations ($\sim 4 \mu\text{Jy}$ at 5 keV and photon index ~ 2.7). Time variation of the hard tail is the possible explanation [see also Urry (1986) and Bezler et al. (1988)]. Many samples of high-quality spectra of BL Lac objects would further constrain the nature of the hard tail. So far energy spectra were obtained with Ginga for two other BL Lac objects, H0323+022 and Mrk 421, and neither exhibits a hard tail (Ohashi and Makino 1988). Therefore, the occurrence of the hard tail may be rather rare.

The synchrotron self-Compton (SSC) model for the continuum emission from radio through X-ray bands was discussed for PKS 2155–304 by Urry and Mushotzky (1982). Using the shortest time scale of variability (luminosity doubling time of 2 hr) reported by Morini et al. (1986) and the redshift factor $z=0.117$ (Bowyer et al. 1984), one obtains a lower limit of the angular size of the X-ray source to be $8.5 \times 10^{-5} \delta$ milli-arcsec (mas), where δ is the kinematical Doppler factor with the same definition by Urry and Mushotzky (1982). Using this angular size and the spectral parameters used by Urry and Mushotzky (1982), in particular the synchrotron self absorption frequency ν_m and the energy flux at ν_m to be 1 GHz and 0.3 Jy, respectively, one needs the Doppler factor δ of more than 400 to reduce the self-Compton flux within the present upper limit of $0.3 \mu\text{Jy}$ at 20 keV. Such a Doppler factor is unreasonably high. This will be relaxed if ν_m is 2×10^3 GHz and the energy flux at ν_m is 0.1 Jy. In this case, the lower limit of δ is 6 and the lower limit of the angular size is 5×10^{-4} mas. The magnetic field is 12 G and the energy densities of the magnetic field, relativistic electrons and synchrotron photons become nearly the same at about 5 erg cm^{-3} . The light crossing time and the cooling time of electrons are 22 hr and 14 hr, respectively. These values seem physically acceptable and suggest that the radio emitting region ($\nu < 2 \times 10^3$ GHz) would be larger than the optical and X-ray emitting region [see e.g., Ghisellini et al. (1985) for inhomogeneous SSC models]. However, no observational data is available in the wavelength region from 2×10^{11} to 10^{14} Hz to date. If correlations in the variability are observed in various wavelength regions, they would give us crucial information on the emission mechanism and the geometry of the BL Lac sources.

The authors are grateful to all the members of the Ginga Team in both Japan and UK for their various forms of support throughout the observations and the data analysis. T.O. thanks Meg Urry for many useful comments on the manuscript.

References

- Agrawal, P. C., Singh, K. P., and Riegler, G. R. 1987, *Monthly Notices Roy. Astron. Soc.*, **227**, 525.
- Allen, C. W. 1973, *Astrophysical Quantities*, 3rd ed. (The Athlone Press, London), p. 31.
- Bezler, M., Gruber, D. E., and Rothschild, R. E. 1988, *Astrophys. J.*, **334**, 995.
- Bowyer, S., Brodie, J., Clarke, J. T., and Henry, J. P. 1984, *Astrophys. J. Letters*, **278**, L103.
- Canizares, C. R., and Kruper, J. 1984, *Astrophys. J. Letters*, **278**, L99.
- Cavallo, G., and Rees, M. J. 1978, *Monthly Notices Roy. Astron. Soc.*, **183**, 359.
- Fabian, A. C. 1979, *Proc. Roy. Soc. London, Ser. A*, **366**, 449.
- George, I. M., Warwick, R. S., and Bromage, G. E. 1988, *Monthly Notices Roy. Astron. Soc.*, **232**, 793.
- Ghisellini, G., Maraschi, L., and Treves, A. 1985, *Astron. Astrophys.*, **146**, 204.
- Hayashida, K., Inoue, H., Koyama, K., Awaki, H., Takano, S., Tawara, Y., Williams, O. R., Denby, M., Stewart, G. C., Turner, M. J. L., Makishima, K., and Ohashi, T. 1989, *Publ. Astron. Soc. Japan*, **41**, 373.
- Inoue, H. 1985, *Japan-U.S. Seminar on Galactic and Extragalactic Compact X-Ray Sources*, ed. Y. Tanaka and W. H. G. Lewin (Institute of Space and Astronautical Science, Tokyo), p. 283.
- Kellermann, K. I. 1966, *Astrophys. J.*, **146**, 621.
- Koyama, K., Inoue, H., Tanaka, Y., Awaki, H., Takano, S., Ohashi, T., and Matsuoka, M., 1989, *Publ. Astron. Soc. Japan*, **41**, 731.
- Koyama, K., Makishima, K., Tanaka, Y., and Tsunemi, H. 1986, *Publ. Astron. Soc. Japan*, **38**, 121.
- Krolik, J. H., Kallman, T. R., Fabian, A. C., and Rees, M. J. 1985, *Astrophys. J.*, **295**, 104.
- Madejski, G. M. 1985, Ph. D. Thesis, Harvard University.
- Makino, F., and the ASTRO-C team 1987, *Astrophys. Letters Commun.*, **25**, 223.
- Maraschi, L., Tagliaferri, G., Tanzi, E. G., and Treves, A. 1986, *Astrophys. J.*, **304**, 637.
- Matsuoka, M., Ikegami, T., Inoue, H., and Koyama, K. 1986, *Publ. Astron. Soc. Japan*, **38**, 285.
- Morini, M., Chiappetti, L., Maccagni, D., Maraschi, L., Molteni, D., Tanzi, E. G., Treves, A., and Wolter, A. 1986, *Astrophys. J. Letters*, **306**, L71.
- Mushotzky, R. F., Boldt, E. A., Holt, S. S., and Serlemitsos, P. J. 1979, *Astrophys. J. Letters*, **232**, L17.
- Ohashi, T. 1988, in *Physics of Neutron Stars and Black Holes*, ed. Y. Tanaka, (Universal Academy Press, Tokyo), p. 301.
- Ohashi, T., and Makino, F. 1988, in *Physics of Neutron Stars and Black Holes*, ed. Y. Tanaka (Universal Academy Press, Tokyo), p. 361.
- Snyder, W. A., Davidsen, A. F., Wood, K., Kinzer, R., Smathers, H., Shulman, S., Meekins, J. F., Yentis, D. J., Evans, W. D., Byram, E. T., Chubb, T. A., Friedman, H., and Margon, B. 1980, *Astrophys. J. Letters*, **237**, L11.
- Stein, W. A., O'Dell, S. L., and Strittmatter, P. A. 1976, *Ann. Rev. Astron. Astrophys.*, **14**, 173.
- Treves, A., Morini, M., Chiappetti, L., Fabian, A., Falomo, R., Maccagni, D., Maraschi, L., Tanzi, E. G., and Tagliaferri, G. 1989, *Astrophys. J.*, **341**, 733.
- Tucker, W. H. 1975, *Radiation Processes in Astrophysics* (MIT Press, Cambridge), p. 111.
- Turner, M. J. L., Thomas, H. D., Patchett, B. E., Reading, D. H., Makishima, K., Ohashi, T., Dotani, T., Hayashida, K., Inoue, H., Kondo, H., Koyama, K., Mitsuda, K., Ogawara, Y., Takano, S., Awaki, H., Tawara, Y., and Nakamura, N. 1989, *Publ. Astron. Soc. Japan*, **41**, 345.
- Urry, C. M. 1986, in *The Physics of Accretion onto Compact Objects*, ed. K. O. Mason, M. G. Watson, and N. E. White (Springer-Verlag, Berlin), p. 357.
- Urry, C. M., Kondo, Y., Hackney, K. R. H., and Hackney, R. L. 1988, *Astrophys. J.*, **330**, 791.
- Urry, C. M., and Mushotzky, R. F. 1982, *Astrophys. J.*, **253**, 38.
- Urry, C. M., Mushotzky, R. F., and Holt, S. S. 1986, *Astrophys. J.*, **305**, 369.
- Wang, B., Inoue, H., Koyama, K., Tanaka, Y., Hirano, T., and Nagase, F. 1986, *Publ. Astron. Soc. Japan*, **38**, 685.